

# Steroid Inhibition of Rat Neuronal Nicotinic $\alpha 4\beta 2$ Receptors Expressed in HEK 293 Cells<sup>1</sup>

KEN PARADISO, KIMBERLEY SABEY, ALEX S. EVERS, CHARLES F. ZORUMSKI, DOUGLAS F. COVEY, and JOE HENRY STEINBACH

Departments of Anesthesiology (K.P., K.S., A.S.E., J.H.S.), Psychiatry (C.F.Z.), and Molecular Biology and Pharmacology (D.F.C.), Washington University School of Medicine, St. Louis, Missouri

Received February 23, 2000; accepted May 11, 2000

This paper is available online at <http://www.molpharm.org>

## ABSTRACT

Steroids, in addition to regulating gene expression, directly affect a variety of ion channels. We examined the action of steroids on human embryonic kidney 293 cells stably transfected to express rat  $\alpha 4\beta 2$  neuronal nicotinic receptors. Each steroid that was tested inhibited acetylcholine responses from these receptors, with slow kinetics requiring seconds for block to develop and recover. The action of one steroid [3 $\alpha$ ,5 $\alpha$ ,17 $\beta$ -3-hydroxyandrostane-17-carbonitrile (ACN)] was studied in detail. Block showed enantioselectivity, with an IC<sub>50</sub> value of 1.5  $\mu$ M for ACN and 4.5  $\mu$ M for the enantiomer. Inhibition curves had Hill slopes larger than 1, indicating more than one binding site per receptor. Block did not require intracellular compounds containing high-energy phosphate bonds and was not affected by analogs of GTP, suggesting that the mechanism does not

require the activation of second messengers. Block did not appear to be strongly selective between open and closed channel states or to involve changes in desensitization. A comparison of different steroids showed that a  $\beta$ -orientation of groups at the 17 position produced more block than  $\alpha$ -orientated diastereomers. The stereochemistry at the 3 and 5 positions was less influential for block of  $\alpha 4\beta 2$  nicotinic receptors, despite its importance for potentiation of  $\gamma$ -aminobutyric acid<sub>A</sub> receptors. The ability of steroids to block neuronal nicotinic receptors correlated with their ability to produce anesthesia in *Xenopus* tadpoles, but the concentrations required for inhibition are generally greater. Similarly, the concentrations of endogenous neurosteroids required to inhibit receptors are larger than estimates of brain concentrations.

In recent years, a number of studies have shown that steroids can have a rapid action in the brain and can produce clinical anesthesia as well as affecting mood and performance in humans. These rapid actions are apparently mediated by binding to membrane proteins, including ligand-gated ion channels. A variety of steroids can enhance activation of the  $\gamma$ -aminobutyric acid type A (GABA<sub>A</sub>) receptor by GABA and may cause direct gating of this receptor (reviewed in Lambert et al., 1995). Certain sulfated steroids block GABA<sub>A</sub> receptors (Majewska and Schwartz, 1987) and can also enhance the activity of *N*-methyl-D-glutamate-type glutamate receptors (Park-Chung et al., 1997). Finally, steroids are known to inhibit the muscle (Gillo and Lass, 1984) and neuronal (Bertrand et al., 1991; Ke and Lukas, 1996) nicotinic receptor.

The most prevalent nicotinic receptor in the brain is composed of the  $\alpha 4$  and  $\beta 2$  subunits, which form the high-affinity

nicotine binding component. The physiological role of this particular subunit combination is not fully understood, but it is known that the numbers in the brain are altered by chronic nicotine exposure and in some conditions, including Alzheimer's disease (reviewed in Role and Berg, 1996). In general, nicotinic receptors in the brain may serve as presynaptic receptors that modulate transmitter release (reviewed in McGehee and Role, 1996). Steroids can inhibit the neuronal nicotinic  $\alpha 4\beta 2$  receptor, and it has been suggested that it may be a target for rapid steroid actions in the brain (Bertrand et al., 1991). Previous studies on neuronal nicotinic receptors have indicated that there is some specificity for steroid structure in producing inhibition and that steroids act from the external solution, because progesterone covalently coupled to bovine serum albumin can inhibit (Valera et al., 1992; Ke and Lukas, 1996). Because neuronal nicotinic receptors and GABA<sub>A</sub> receptors are members of the same extended gene family, it is also of interest to compare the structural requirements for block by steroids, in one case, and potentiation, in

<sup>1</sup> This work was supported by National Institutes of Health Grants P01-GM47969 (J.H.S., D.F.C., A.E., C.Z.) and R01-NS22356 (J.H.S.) J.H.S. is the Russell and Mary Shelden Professor of Anesthesiology.

**ABBREVIATIONS:** GABA,  $\gamma$ -aminobutyric acid; LRR, loss of righting reflex; B163, (3 $\alpha$ ,5 $\beta$ ,17 $\alpha$ )-3-hydroxyandrostane-17-carbonitrile; B164, (3 $\alpha$ ,5 $\beta$ ,17 $\beta$ )-3-hydroxyandrostane-17-carbonitrile; ECN, (3 $\beta$ ,5 $\alpha$ ,17 $\beta$ )-17-hydroxyestrane-3-carbonitrile; B260, (3 $\beta$ ,5 $\beta$ ,17 $\beta$ )-3-hydroxyandrostane-17-carbonitrile; B372, (3 $\beta$ ,5 $\alpha$ ,17 $\beta$ )-3-hydroxyandrostane-17-carbonitrile; AND, (3 $\alpha$ ,5 $\alpha$ ,17 $\beta$ )-androstane-3,17-diol;  $\beta$ EST, 17 $\beta$ -estradiol;  $\alpha$ EST, 17 $\alpha$ -estradiol; 3 $\alpha$ 5 $\alpha$ P, (3 $\alpha$ ,5 $\alpha$ ,17 $\beta$ )-3-hydroxypregnan-20-one; DHEAS, dehydroepiandrosterone sulfate; PROG, progesterone; ACN, (3 $\alpha$ ,5 $\alpha$ ,17 $\beta$ )-3-hydroxyandrostane-17-carbonitrile.

surface of the  $\beta 2$  subunit. The cells used in this study had been sequentially selected six times but had not been cloned. The cDNAs for the rat neuronal nicotinic subunits were kindly provided by Dr. J. Patrick (Baylor College of Medicine, Houston, TX).

**Electrophysiology of Nicotinic Responses.** Cells were plated onto 35- or 60-mm tissue culture dishes and used within 4 days after plating. Recordings were made in an extracellular saline composed of 140 mM NaCl, 1 mM MgCl<sub>2</sub>, 2 mM CaCl<sub>2</sub>, 10 mM HEPES, 5 mM KCl, and 10 mM glucose, pH 7.3. The internal solution was composed of 4 mM NaCl, 4 mM MgCl<sub>2</sub>, 0.5 mM CaCl<sub>2</sub>, 10 mM HEPES, 5 mM EGTA, and 140 mM CsCl, pH 7.3. Standard methods were used to record currents in the whole-cell configuration. Records were filtered with a four-pole Bessel filter (Frequency Devices, Haverhill, MA) and directly digitized by a PC clone computer using a Digidata interface (Axon Instruments, Foster City, CA). Drugs were dissolved in external solution and applied through a three-tube perfusion system (Sabey et al., 1999). The three-tube perfuser provided a solution change around cells attached to the culture substrate with a 10-to-90% time of about 50 ms (data not shown; from the time course of changes in holding current when bath solutions with different ion concentrations were applied to cells). The cell was perfused with extracellular solution continuously between applications of agonists or other drugs. To reduce loss of steroids as a result of sticking to plastics, the perfusion system used glass syringe reservoirs, Teflon tubing, Teflon valves, and quartz perfuser tips.

Unless otherwise noted, chemicals were obtained from Sigma Chemical Co. (St. Louis, MO).

Steroids were prepared as 10 mM stocks in DMSO and diluted into extracellular solution. The highest concentration of DMSO in the final solution was 0.3% (42 mM). At the usual test dose of steroid (3  $\mu$ M), the DMSO concentration was 4.2 mM, and control applications of DMSO had no significant effect on the response to acetylcholine (Table 1). At 42 mM, the response was reduced to  $0.93 \pm 0.11$  (mean  $\pm$  S.D.,  $N = 6$ ), which also not significantly different from control applications of bath solution.

The amplitude of a response was taken as the mean of a short interval centered at the peak response, using Clampfit (Axon Instruments). The response of a cell often varied over time. Most often responses initially increased and then decreased at longer times of recording (“ran down”). The decline was an experimental problem because it limited our ability to obtain data from experiments that required long series of drug applications or prolonged wash periods. To control for this variability, drug effects were normalized to the

The table is organized with the compound producing the greatest block (ACN) at the top and that producing the least (bath solution) at the bottom. The structures of the drugs used are shown in Fig. 6. The first column gives the name of the compound. The second column shows the mean residual response to 100  $\mu\text{M}$  acetylcholine after 30-s preexposure to the steroid (all at 3  $\mu\text{M}$  concentration) for *N* cells. The next three columns give the substituent and orientation at the 3, 5, and 17 positions, respectively. The next two columns show the measured  $\text{IC}_{50}$  values and Hill coefficient for inhibition or the calculated  $\text{IC}_{50}$  value (in parentheses). The calculated  $\text{IC}_{50}$  value was estimated from the mean residual current with 3  $\mu\text{M}$  compound ( $\rho$ ) and the mean value for the Hill coefficient for all the blocking curves determined (1.4), using the equation  $\text{IC}_{50} = 1.4 \text{ th root } [(1 - \rho)/\rho] \times 3 \mu\text{M}$ .

Compound	ACh Response	<i>N</i>	3	5	17	IC <sub>50</sub>	Hill <i>n</i>	<i>P</i> versus ACN	<i>P</i> versus DMSO
	<i>mean</i> ± <i>S.D.</i>					<i>μM</i>			
ACN	0.27 ± 0.09	11	αOH	α	βCN	1.64	1.75		***
B164	0.28 ± 0.10	3	αOH	β	βCN	(1.55)		NS	**
B372	0.33 ± 0.10	10	βOH	α	βCN	(1.83)		NS	***
B260	0.46 ± 0.07	3	βOH	β	βCN	(2.69)		*	**
PROG	0.50 ± 0.13	6	O	x	βCH <sub>3</sub> CO	3.03	1.22	**	***
<i>ent</i> -ECN	0.54 ± 0.18	5	αCN	β	αOH	(3.37)		*	**
ECN	0.56 ± 0.17	5	βCN	α	βOH	(3.58)		*	**
AND	0.57 ± 0.10	3	αOH	α	βOH	(3.61)		*	**
<i>ent</i> -ACN	0.61 ± 0.18	8	βOH	β	αCN	4.64	1.39	**	**
B163	0.66 ± 0.20	5	αOH	β	αCN	(4.76)		*	**
βEST	0.69 ± 0.04	4	OH	x	βOH	(5.30)		***	***
DHEAS	0.76 ± 0.12	4	βSO <sub>4</sub>	x	O	(6.96)		**	*
αEST	0.79 ± 0.12	15	OH	x	αOH	11.7	1.15	***	**
3α5αP	0.84 ± 0.08	4	αOH	α	βCH <sub>3</sub> CO	12.3	1.55	***	**
DMSO	0.96 ± 0.08	7						***	
Bath	1.03 ± 0.16	19						***	NS

The last two columns give the probabilities that the residual response seen for a given drug was the same as that seen with 3  $\mu$ M ACN or 0.03% DMSO, respectively: NS:  $P > .05$ , \*  $P < .05$ , \*\*  $P < .01$ , \*\*\*  $P < .001$  (two-tailed  $t$  tests assuming unequal variances).

interpolated value of controls taken before and after the test response.

**Steroid Action on GABA<sub>A</sub> Receptors.** The ability of steroids to act on GABA<sub>A</sub> receptors was examined as described (Wittmer et al., 1996). In brief, GABA (2  $\mu$ M) or GABA (2  $\mu$ M) plus steroid (10  $\mu$ M) were applied to voltage-clamped cultured rat hippocampal neurons using matched puffer pipettes. Data on potentiation are presented as the ratio of the peak response in the presence of GABA plus steroid to the response to GABA alone (no potentiation is 1.0 and block is <1).

**Tadpole Loss of Righting Reflex (LRR).** The tadpole LRR assay was conducted as described (Wittmer et al., 1996). In brief, groups of 10 tadpoles were exposed to various concentrations of steroid in Ringer's solution. After equilibration at room temperature for 3 h, tadpoles were flipped onto their backs using a smooth glass rod. LRR was defined as failure of the tadpole to right itself within 5 s after being turned over. Reversibility was determined by returning the tadpoles to normal Ringer's solution and demonstrating that they recovered normal righting reflexes. The concentrations of anesthetic agents producing LRR in half the tadpoles correlate well with concentrations necessary to produce anesthesia in mammals (Tonner et al., 1992; Franks and Lieb, 1993).

**Data Analysis.** All values are presented and shown in graphs as the arithmetic mean  $\pm$  1 S.D., based on  $N$  observations. Concentration-effect relationships were analyzed in Excel (Microsoft, Redmond, WA) and SigmaPlot (SSPS, Chicago, IL). Comparisons of the relative ability of steroids to block responses were made using the unpaired  $t$  test assuming unequal variances.

**Fitting of Kinetic Models.** Fitting of the time course of block by 10  $\mu$ M ACN and recovery from block by 10  $\mu$ M ACN was performed with SCOP (Simulation Resources, Berrien Springs, MI), using numerical solution of the kinetic models. The models were implemented in SCOP using the "kinetic" form of model entry, in which transition rates were entered and quality of fit was judged from  $\chi^2$ . As presented in *Results*, four simple kinetic models were used in the analysis. For each model, it was assumed that there were an integral number ( $M$ ) of binding sites for steroid on each receptor. The sites were assumed to be identical and independent for binding steroid.

The first pair of models was two variants of a simple occupancy blocking model: Occ1 and OccM. For each site, a simple binding interaction between receptor (R) and steroid (S) was assumed to occur ( $R + S \rightleftharpoons RS$ ), with an association rate constant  $k_{+b}$  and dissociation rate constant  $k_{-b}$ . The microscopic dissociation constant at each site is  $K_d = k_{-b}/k_{+b}$ . For both Occ1 and OccM, it was assumed that a blocked receptor was completely inactive. Occ1 and OccM differ in a single assumption: for Occ1, it was assumed that the receptor was blocked when only a single site was occupied. In other words, only R was activatable, whereas RS, RS<sub>2</sub>, . . . , RS<sub>M</sub> were all blocked. In contrast, for OccM, only RS<sub>M</sub> was blocked, whereas R, RS, . . . , RS<sub>M-1</sub> were all activatable.

The other two schemes were conformational change models in which it was assumed that ACN bound and unbound rapidly and a slower conformational change occurred after the blocking site or sites were occupied to produce block [ $R + S \rightleftharpoons RS \rightleftharpoons BS$ ], where B now indicates a blocked receptor. The two variations of a conformational change model examined were Con1, in which the conformational change leading to block can occur when one or more sites were occupied by ACN, and ConM, in which all  $M$  sites must be occupied before the change can occur. These models have two additional parameters: the rate constant for development of block ( $k_F$ ) and the rate constant for recovery ( $k_R$ ). The forward blocking equilibrium  $Z$  ( $Z = k_F/k_R$ ) describes the steady-state efficacy of the blocking step, which must be high to provide the level of block observed. In performing the fits, the dissociation rate ( $k_{-b}$ ) was fixed at a high value (100 s<sup>-1</sup>) to ensure that the assumption of rapid binding reactions was maintained, whereas the association rate constant ( $k_{+b}$ ) was varied to optimize the value for the dissociation constant.

The analysis proceeded as follows. In all cases, individual data

points were used rather than the averaged values shown (for clarity) in the figures. Each data point was weighted equally. The predictions of the models were fit to the data for onset and offset of block by 10  $\mu$ M ACN, for various assumed values of  $M$ . At this point, some models clearly failed; for example, with  $M = 1$ , the predictions for either occupancy or conformational models were clearly worse judged by eye and  $\chi^2$  values were larger. The second step was to use the predicted values for rate constants to predict the steady-state block. Again, models with  $M = 1$  clearly failed as they predicted IC<sub>50</sub> values of 0.3  $\mu$ M ACN and 0.6  $\mu$ M ACN (experimental value 1.6  $\mu$ M) for the conformational and occupancy models, respectively. Similarly, with assumed values for  $M = 2, 3$ , or 5, both the Con1 and OccM models predicted IC<sub>50</sub> values of 0.3 to 0.6  $\mu$ M. Accordingly, these models were discarded as unable to describe the actions of ACN. The final test was to use the values of rate constants to predict the onset of block by 1  $\mu$ M ACN for the remaining models. Overall, the sets of models ranked as follows (in terms of increasing  $\chi^2$  values, so small values are better). The results obtained with the Occ1 model fitting the 10  $\mu$ M data were: with an assumed  $M = 2 < M3 < M5 < M8$ ; fitting the 1  $\mu$ M data:  $M8 = M5 < M3 < M2$ ; and fitting the steady-state block,  $M5$  (IC<sub>50</sub> = 1.5  $\mu$ M) =  $M8$  (IC<sub>50</sub> = 1.5  $\mu$ M) <  $M3$  (IC<sub>50</sub> = 1.2  $\mu$ M) <  $M2$  (IC<sub>50</sub> = 1.0  $\mu$ M). Overall, Occ1 with  $M > 3$  appears superior among this set of fits. The results obtained with the ConM model fitting the 10  $\mu$ M data were:  $M5 = M3 = M2$ ; fitting the 1  $\mu$ M data,  $M2 < M3 < M5$ ; and fitting the steady-state block,  $M2$  (IC<sub>50</sub> = 1.2  $\mu$ M) <  $M3$  (IC<sub>50</sub> = 1.9  $\mu$ M) <  $M5$  (IC<sub>50</sub> = 2.5  $\mu$ M). Overall, ConM with  $M = 2$  appears superior among this set of fits. Comparing between Occ1 and ConM, Occ1 ( $M = 5$ ) had a smaller  $\chi^2$  value than ConM ( $M = 2$ ) for descriptions of the 1  $\mu$ M onset data and the steady-state blocking curve and larger  $\chi^2$  for fitting the 10  $\mu$ M onset and offset data. Hence, it is not apparent that one model provides a significantly better description of the data.

A final independent set of equations was used to fit the steady-state blocking curves, derived from the predictions of the kinetic models Occ1 and ConM. These equations relate the fractional response to the concentration of steroid: for Occ1,  $Y = \{1/(1 + [S]/K_d)\}^M$ , and for ConM,  $Y = (1 + [S]/K_d)^M / (1 + [S]/K_d)^M + Z([S]/K_d)^M$ , where  $S$  indicates steroid and other terms are defined earlier. When  $M$  is an integer, these equations are predictions of the kinetic models. They were implemented, however, with  $K_d$ ,  $M$ , and  $Z$  (when applicable) as free parameters and  $M$  was not constrained to assume integer values. For the model derived from Occ1, the fits converged well to provide estimates  $K_d = 11$   $\mu$ M and  $n = 5.02$ . For the model derived from ConM, the fit was not well constrained; the best fitting value for  $n$  was about 1.36, whereas the estimates for  $Z$  and  $K_d$  both increased indefinitely while maintaining a constant ratio. This behavior can be predicted from the form of the equation describing steady-state block, because the equation approaches the Hill equation (eq. 1 in *Results*) when the  $K_d$  becomes large compared with the range of concentrations studied. In that case, the parameters  $Z$  and  $K_d$  appear only as a ratio and cannot be determined independently.

## Results

**Time Course of Steroid Inhibition of Responses.** The steroid ACN reversibly reduced the acetylcholine-elicited response of cells expressing nicotinic receptors composed of rat  $\alpha 4$  and  $\beta 2$  subunits (Fig. 1; see also Sabey et al., 1999). The block developed and reversed slowly. The slow kinetics of inhibition by ACN was not due to perfusion artifacts, as the response to acetylcholine was much more rapid (see Fig. 1).

The relative response amplitudes after various times of preincubation with steroid are shown in Fig. 2A, whereas Fig. 2B shows the recovery from steroid block after various intervals of washing. The onset of block was faster and the extent of block was greater when 10  $\mu$ M ACN was applied than when 1  $\mu$ M ACN was used. Because the rate of block by



ACN was slow compared with the rate of desensitization at high concentrations of acetylcholine, it was difficult to measure block by coapplying steroid with acetylcholine. However, we could examine the onset of block by coapplying a low concentration of acetylcholine (1  $\mu\text{M}$ ) to minimize desensitization and a high concentration of ACN (10  $\mu\text{M}$ ) to increase the rate of block. As shown in Fig. 3, the development of block agreed well when measured either by various durations of

preapplication or by simultaneous application of acetylcholine and ACN.

Our subsequent studies usually used preapplication times of 30 s for steroids, although at high concentrations, we sometimes used 10-s preapplications. Either time is sufficient to reach full block.

**Concentration-Effect Relationship for ACN.** The relationship between inhibition and the concentration of ACN is shown in Fig. 4. The inhibition data were fit with eq. 1:

$$Y = 1/[1 + ([S]/IC_{50})^n] \quad (1)$$

where  $IC_{50}$  is the concentration of steroid (S) producing half-reduction in the response and  $n$  is the Hill coefficient. The fit parameters for the data in Fig. 4 (responses elicited with 100  $\mu\text{M}$  acetylcholine) were an  $IC_{50}$  value of 1.65  $\mu\text{M}$  and an  $n$  value of 1.8. We usually used 100  $\mu\text{M}$  acetylcholine to test the responsiveness of cells. However, we also tested the ability of ACN to block responses elicited by 1  $\mu\text{M}$  acetylcholine and estimated that the  $IC_{50}$  was about 1.7  $\mu\text{M}$  (results not shown).

These data demonstrate that the blocking ability of ACN is similar when either 1 or 100  $\mu\text{M}$  acetylcholine was used to elicit a response. However, they cannot be interpreted in terms of competitive interactions because the action of ACN is so slow that equilibrium would not be reached in the presence of acetylcholine. Previous work, however, has found that ACN does not affect the binding of radiolabeled cytosine to homogenates prepared from these cells (Sabey et al., 1999), which indicates that ACN does not occlude the agonist binding site at equilibrium.

**Properties of Inhibition by ACN.** A hydrophobic molecule such as ACN could produce effects mediated by a number of mechanisms, including indirect actions produced by perturbations of the lipid bilayer. One test for the site of action is to determine whether the mirror image of the compound (the enantiomer) has identical effects. The two enantiomers will have identical physical properties, including lipid solubility, but will differ in stereospecific interactions

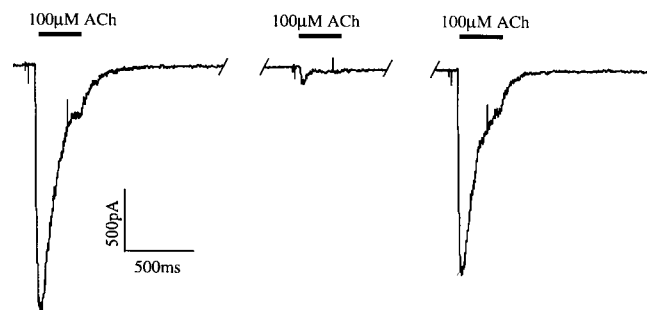


**Fig. 1.** The steroid ACN reversibly blocks responses to 100  $\mu\text{M}$  acetylcholine. The traces show responses of a cell to 100  $\mu\text{M}$  acetylcholine before (left) and 60 s after (right) a response elicited immediately after a 30-s exposure to 10  $\mu\text{M}$  ACN (middle). Responses were recorded at  $-100$  mV.

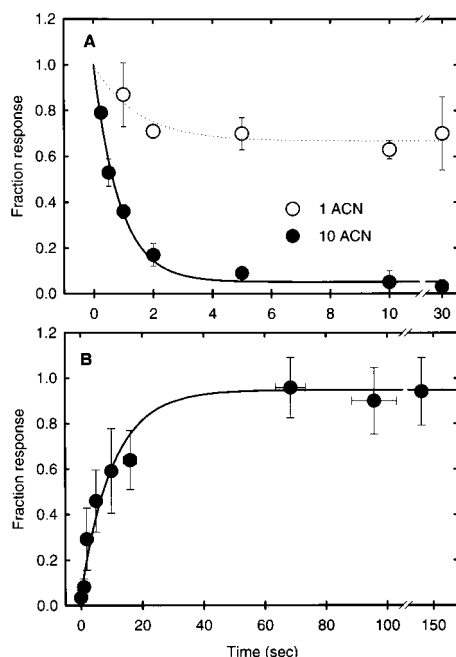


**Fig. 2.** Time course of inhibition and recovery. A, fraction of control current recorded immediately after exposure to 1  $\mu\text{M}$  ACN ( $\circ$ , dotted line) or 10  $\mu\text{M}$  ACN ( $\bullet$ , solid line) for the indicated time. Responses were assayed with 100  $\mu\text{M}$  acetylcholine. Each point shows the arithmetic mean  $\pm$  1 S.D. for 2 to 19 cells, whereas the lines show the fits of single exponential functions declining from 1 to a constant residual current. B, fraction of control current recorded after a 30-s exposure to 10  $\mu\text{M}$  ACN followed by a wash with normal bath solution for the indicated time. Responses assayed with 1  $\mu\text{M}$  acetylcholine. Each point shows the arithmetic mean  $\pm$  1 S.D. for 9 to 39 cells, whereas the line shows a single exponential rising from a constant to a final steady level. Note that zero time is offset from the ordinate. We will analyze the time courses further later, but note here that the time for development of half-maximal inhibition was longer when 1  $\mu\text{M}$  ACN was used than with 10  $\mu\text{M}$  ACN. When the data were fit with a single exponential function declining to a constant level, the half-time with 1  $\mu\text{M}$  ACN was 1 s (final level, 0.67), whereas with 10  $\mu\text{M}$  ACN, it was 0.6 s (final level, 0.05). When the data for recovery were fit with a single exponential, the time for half-recovery was 7 s (initial value, 0.05; final value, 0.95).

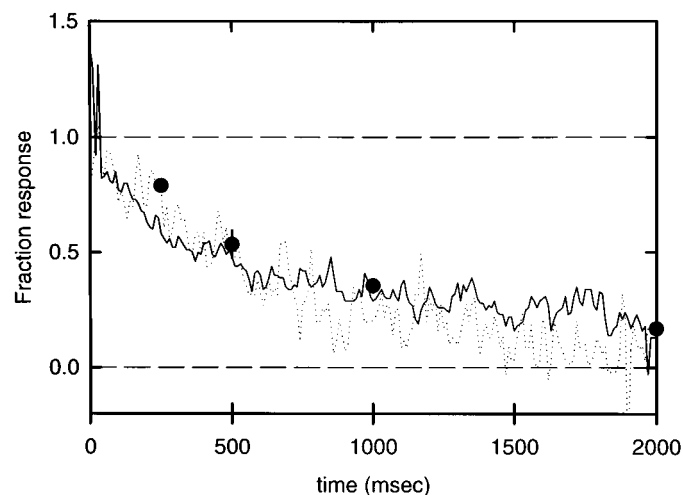


**Fig. 3.** Time course of inhibition. The traces show the currents for two cells that were exposed to 1  $\mu\text{M}$  acetylcholine plus 10  $\mu\text{M}$  ACN for 2 s, normalized to the currents recorded in the same cells in response to 1  $\mu\text{M}$  acetylcholine alone (one cell continuous line, the other dotted). Superimposed on the traces are the mean values shown in Fig. 2A for development of inhibition during preexposure to 10  $\mu\text{M}$  ACN alone. The time courses match very well.

with chiral sites (e.g., a binding site on a protein). The data shown in Fig. 4 demonstrate enantioselectivity in the inhibition of responses elicited by 100  $\mu$ M acetylcholine. The data with *ent*-ACN were fit by eq. 1 with parameters of  $IC_{50} = 4.6$   $\mu$ M and  $n = 1.4$ . The block with 3  $\mu$ M ACN ( $0.27 \pm 0.09$  residual current,  $N = 11$ ) was significantly larger than that with 3  $\mu$ M *ent*-ACN ( $0.61 \pm 0.18$ ,  $N = 8$ ;  $P = .001$ ).

The results have demonstrated that block by ACN is relatively slow to develop and reverse. We examined the possibility that ACN might act by inducing or stabilizing a desensitized state of the receptor. Desensitization is a phenomenon in which the response to a constant concentration of agonist wanes; the traces in Fig. 1 show the desensitization during the application of 100  $\mu$ M acetylcholine. Desensitization also is produced by applications of nicotine, another nicotinic agonist (K. Paradiso, in preparation).

A possible interaction between block by ACN and desensitization was examined by measuring the recovery of responses from inhibition. The protocol was to pretreat a cell for 13 s with 10  $\mu$ M ACN. In the control case, all 13 s were with 10  $\mu$ M ACN alone; in the experimental case, the initial 10 s were with 10  $\mu$ M ACN, whereas the final 3 s were with 10  $\mu$ M ACN coapplied with 100  $\mu$ M nicotine. At the end of the 13-s exposure, the cell was washed for 10 s with bath solution, and the response was tested. After the recovery period, cells treated with ACN alone had a recovered response of  $0.39 \pm 0.10$  ( $N = 4$ ), whereas cells treated with both ACN and nicotine had a smaller recovered response of  $0.19 \pm 0.08$  ( $N = 4$ ;  $P = .004$ ). Accordingly, cells could be desensitized by nicotine even when the responses were blocked by ACN. We also applied 100  $\mu$ M nicotine alone for 3 s, washed for 10 s, and then tested. In this case, the recovered response was  $0.32 \pm 0.16$  ( $N = 5$ ; not significantly different from the recovered response after ACN and nicotine). The null hypothesis is that desensitization and block by ACN are independent. If there is no interaction and inhibition is essentially complete by each mechanism, then the amount of recovery from the combined actions of ACN and desensitization should be equal to the product of the recovery from the two processes

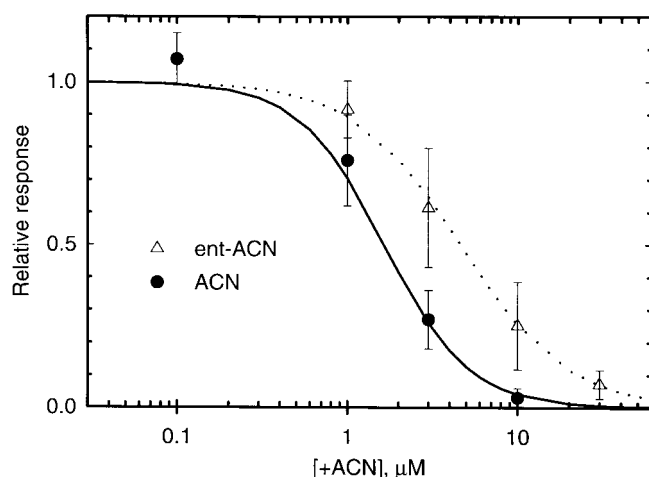


**Fig. 4.** Inhibition by ACN and *ent*-ACN. The fraction of control current remaining after a 30-s application of ACN (●, solid line) or *ent*-ACN (△, dotted line) is shown. The lines show the fits of eq. 1 to the data; for data with ACN, parameter values are  $IC_{50} = 1.6$   $\mu$ M,  $n = 1.8$ , and with *ent*-ACN, they are  $IC_{50} = 4.6$   $\mu$ M and  $n = 1.4$ . Each point shows the arithmetic mean  $\pm$  1 S.D. for 3 to 19 cells. Responses assayed using 100  $\mu$ M acetylcholine.

separately. In the present data, (ACN alone)  $\times$  (nicotine alone) =  $(0.39) \times (0.32) = 0.13 \pm 0.07$  (calculated standard deviation). The predicted residual response is less than the observed combined effect of 0.19, but the small difference suggests that receptors blocked by ACN desensitize essentially normally and that desensitized receptors with ACN bound recover essentially normally.

The possibility that the slow action of ACN might be mediated by binding to a separate receptor for the steroid, followed by activation of a second messenger pathway that modulated the response of the nicotinic receptor, seems unlikely. First, the intracellular solutions contained no added ATP or other high-energy substrates. When cells were perfused with intracellular solutions containing 5 mM AMP-PNP (a nonhydrolyzable analog of ATP, to swamp residual ATP), block by a 10-s preapplication of 10  $\mu$ M ACN was unaffected (in the presence of 5 mM AMP-PNP, the residual response was  $0.09 \pm 0.04$  ( $N = 4$ ), whereas in cells recorded on the same day with control intracellular solution, the residual response was  $0.10 \pm 0.04$  ( $N = 3$ ). Second, the involvement of a GTP-binding protein is unlikely, because inclusion of guanosine-5'-O-(2-thio)diphosphate or guanosine-5'-O-(3-thio)triphosphate had little effect on the inhibition produced by a 10-s preapplication of 10  $\mu$ M ACN. When cells were perfused with intracellular solution containing 2 mM guanosine-5'-O-(2-thio)diphosphate, the response amplitude was reduced to  $0.07 \pm 0.01$  ( $N = 3$ ), whereas with intracellular solution containing 0.2  $\mu$ M guanosine-5'-O-(3-thio)triphosphate, the response was reduced to  $0.07 \pm 0.02$  ( $N = 3$ ). These values did not differ from responses recorded on the same days with control intracellular solutions ( $0.06 \pm 0.05$ ,  $N = 8$ ). These observations indicate that ACN does not act through a second messenger system involving GTP-binding proteins or requiring high-energy phosphate compounds.

**A Simple Kinetic Description of Block by ACN.** Based on the results we have obtained, it seems likely that steroids interact with a specific site on a target protein. It also is likely that a second messenger system is not required for the actions of steroids. Accordingly, it appears that steroids interact directly with the nicotinic receptor. We undertook an initial analysis of our data to determine whether some kinetic mechanisms for block could be ruled out and to make a provisional estimate of the number of steroid binding sites on the receptor. The goal of the analysis was not to provide a definitive statement on the likely mechanism of block.

We used four simple schemes to model the data; two of the schemes were able to describe our data, whereas two were not. For each scheme, it was assumed that there were  $M$  identical and independent binding sites on each receptor. In physical terms, this might mean that there are two sites (one on each  $\alpha$ -subunit) or five sites (one at each subunit-subunit interface). The analysis is described more fully in *Materials and Methods*.

For each model, the time course of the development of and recovery from block by 10  $\mu$ M ACN was fit with the predictions of the particular model with different assumed values for  $M$ . The time courses provide information on the rates of development of block and recovery, as well as the steady-state level reached. Analysis of the kinetics provides a critical test of the applicability of the kinetic scheme used to model the data, because the rate constants can be used to predict the rates of development and steady-state block at all con-

centrations of ACN. The rate constants were then used to predict the time course of the development of block by 1  $\mu\text{M}$  ACN and the steady-state block at different concentrations of ACN. Finally, the predictions of a more general form of each model were used to fit the steady-state blocking curve (see *Materials and Methods*).

Two of the schemes were occupancy models; that is, block was assumed to occur as soon as ACN had bound to the receptor. This is one simplified picture of how ACN might act, in that binding and unbinding are visualized as very slow compared with any other step in the blocking mechanism. The two variations of an occupancy model examined were Occ1, in which block occurs when one or more of the  $M$  sites are occupied, and OccM, in which all  $M$  sites must be occupied. These were particularly simple schemes in that there are only three parameters: the association rate constant ( $k_{+b}$ ), the dissociation rate constant ( $k_{-b}$ ), and the number of sites ( $M$ ). The microscopic dissociation constant at each site is  $K_d = k_{-b}/k_{+b}$ . It was assumed that the blocked receptor is completely inactive.

The other two schemes were conformational change models, in which it was assumed that ACN bound and unbound very rapidly and a slower conformational change occurred after the blocking sites were occupied to produce block. The two variations of a conformational change model examined were Con1, in which the conformational change leading to block can occur when one or more sites were occupied by ACN, and ConM, in which all  $M$  sites must be occupied before the change can occur. These models have two additional parameters: the rate constant for development of block ( $k_F$ ) and the rate constant for recovery ( $k_R$ ). The forward blocking equilibrium  $Z$  ( $Z = k_F/k_R$ ) describes the steady-state efficacy of the blocking step, which must be high to provide the level of block observed.

In brief, neither the OccM model nor the Con1 model could describe the data. In each case, the fit values for the time course of block by 10  $\mu\text{M}$  ACN could not describe the time course of block by 1  $\mu\text{M}$  ACN or the steady-state blocking curve (data not shown; see *Materials and Methods*). In contrast, the Occ1 and ConM models could describe the data reasonably well.

The Occ1 model did not describe the data for assumed values of  $M$  of 1, 2, or 3 (data not shown; see *Materials and Methods*). It did, however, describe the data well for values of  $M$  of 5 (Fig. 5) or more. The estimates for  $k_{+b}$  and  $k_{-b}$  were quite small. For an assumed value of  $M = 5$ ,  $k_{+b}$  is  $2 \times 10^4 \text{ M}^{-1} \text{ s}^{-1}$  and  $k_{-b}$  is  $0.19 \text{ s}^{-1}$ , giving a calculated  $K_d$  of  $9.1 \mu\text{M}$  and a predicted  $\text{IC}_{50}$  of  $1.5 \mu\text{M}$ . (The calculated  $K_d$  is the microscopic dissociation constant for each of the  $M$  sites. The binding of the first molecule of ACN would have an apparent macroscopic dissociation constant of about  $1.9 \mu\text{M}$  for  $M = 5$ .) In addition, the steady-state blocking curve was fit with a generalized model derived from the Occ1 model in which the fitting parameters were the apparent dissociation constant,  $K_d$ , and the power coefficient,  $n$  (see *Materials and Methods*). The fits converged well to provide estimates  $K_d = 11 \mu\text{M}$  and  $n = 5.02$ . The value for the  $K_d$  is consistent with the steady-state parameter predicted from the kinetic analysis, whereas the value for  $n$  suggests the presence of five binding sites on each receptor.

The ConM model could describe the data equally well for an assumed value of  $M$  of 2 (Fig. 5). The description was not

good for  $M = 1$  or greater than 2 (data not shown; see *Materials and Methods*). For an assumed value of  $M = 2$ , the best fitting value for the  $K_d$  was  $7.4 \mu\text{M}$ , for  $k_F$  it was  $0.0036 \text{ s}^{-1}$ , and for  $k_R$  it was  $0.000078 \text{ s}^{-1}$ . The calculated value for  $Z$  was 46, resulting in a residual response of 0.02 at maximal blocking effect, and the predicted  $\text{IC}_{50}$  was  $1.3 \mu\text{M}$ . In addition, the steady-state blocking curve was fit with a generalized model derived from the ConM model in which the fitting parameters were the apparent dissociation constant,  $K_d$ , the blocking equilibrium  $Z$ , and the power coefficient,  $n$ . The fit was not well constrained; the best fitting value for  $n$  was about 1.4, whereas the estimates for  $Z$  and  $K_d$  both tended to

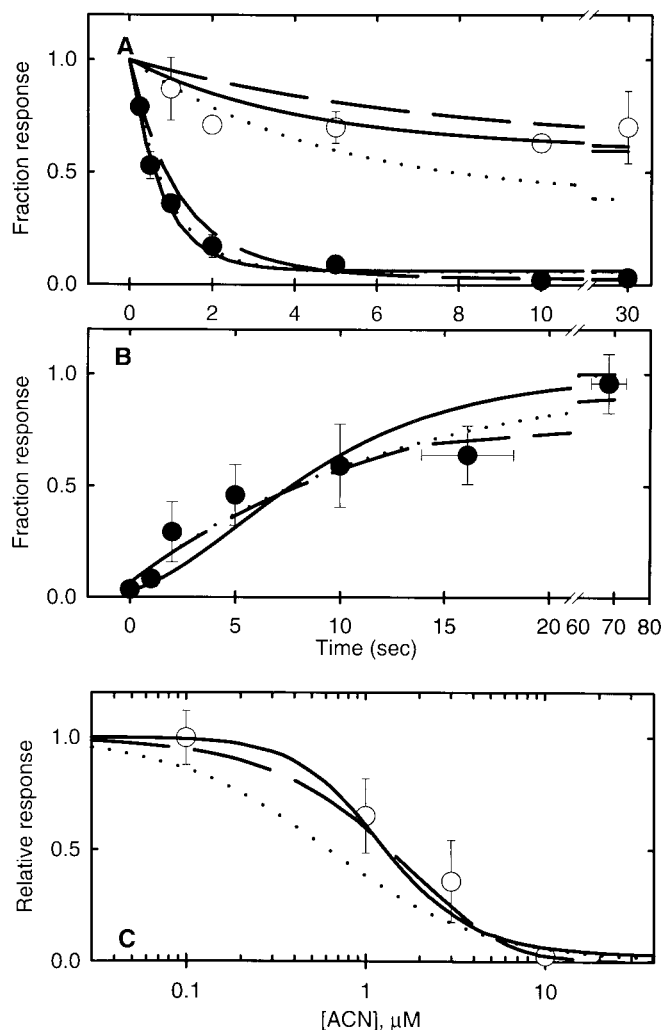


**Fig. 5.** Fits and predictions of simple models for ACN action. The ability of the occupancy model Occ1 (described in *Results*) to describe the data for inhibition by ACN is shown. A, time course for development of inhibition (replotted from Fig. 2A) for 1  $\mu\text{M}$  ACN ( $\circ$ ) and 10  $\mu\text{M}$  ACN ( $\bullet$ ). B, time course for recovery (replotted from Fig. 2B, with altered time base to emphasize the early times). C, dependence of inhibition on the concentration of ACN (pooled data for inhibition of responses measured with 1, 10, or 100  $\mu\text{M}$  acetylcholine; fit parameters for eq. 1 are  $\text{IC}_{50} = 1.6 \mu\text{M}$ ,  $n = 1.4$ ). The superimposed curves show the predictions for the following models: Occ1 with  $M = 1$  (dotted lines), Occ1 with  $M = 5$  (solid lines), or ConM with  $M = 2$  (dashed lines). Note that the assumption of only one site does not describe the data well. In each case the onset (A, solid symbols) and recovery (B) time courses for 10  $\mu\text{M}$  ACN were fit with an assumed value of  $M$ , as described in the text. The parameters were then used to generate the time course of inhibition using 1  $\mu\text{M}$  ACN (A,  $\circ$ ) and the concentration dependence of steady-state block (C), with no free parameters.



increase indefinitely while maintaining a constant ratio. The concentration producing half-maximal inhibition can be predicted from the values of  $Z$ ,  $n$ , and  $K_d$  and approaches  $1.6 \mu\text{M}$ . This behavior can be predicted from the form of the equation describing steady-state block, because the equation approaches eq. 1 when the  $K_d$  becomes large compared with the range of concentrations studied. In that case, the parameters  $Z$  and  $K_d$  appear only as a ratio and cannot be determined independently. In the case of the kinetic analysis, however, the rate constants describing block can be determined.

These simple models can capture many features of the data. Both generate steady-state inhibition curves with a Hill coefficient of greater than 1, and both can describe both the time course and steady-state blocking data with ACN. They both suggest that there are a small number of sites on the receptor, perhaps two or five. They differ in that the conformational change model, ConM, predicts a lag in the onset time course but Occ1 does not, whereas Occ1 predicts a lag in the offset time course but ConM does not. The data show an indication of a lag in the offset (Fig. 5) but not strongly enough to rule out one model. A critical test to distinguish between occupancy and conformational models would be to identify a partial antagonist steroid (one that produced only partial block at maximal effect). In this case, a simple occupancy model would be eliminated, and the equilibrium blocking ratio could be directly determined. A previous report has suggested that  $3\alpha 5\alpha\text{P}$  is only a partial antagonist at chicken  $\alpha 4\beta 2$  receptors expressed in oocytes (Bertrand et al., 1991). In our studies, however, neither this steroid nor others produced partial inhibition of rat  $\alpha 4\beta 2$  receptors (see later). Accordingly, we have not been able to perform this test. The observation of partial antagonism of chicken receptors, however, provides circumstantial support for a conformational change model.

The major consequences of the models in terms of interpretation is that the occupancy model results in very slow rates for association and dissociation of ACN. With Occ1 and an assumed value of  $M = 5$ ,  $k_{+b}$  is  $2 \times 10^4 \text{ M}^{-1} \text{ s}^{-1}$  and  $k_{-b}$  is  $0.19 \text{ s}^{-1}$ . In comparison, the association rate for a diffusion-limited process is expected to be close to  $10^8 \text{ M}^{-1} \text{ s}^{-1}$ . If we assume a  $K_d$  value of  $9 \mu\text{M}$  and an association rate of  $10^8 \text{ M}^{-1} \text{ s}^{-1}$ , the predicted dissociation rate is  $900 \text{ s}^{-1}$ , almost 1000-fold faster than the observed time constant for recovery. In contrast, for the conformational change model, the slow steps are assumed to be the conformational changes. If the occupancy model is applicable, slow binding rates could result from several possible factors; perhaps the steroid must follow a tortuous path to reach its site, or perhaps the site is most often concealed and is revealed only for a very small fraction of the time.

**Structure Activity Relationship.** A number of structurally related steroids were examined with three goals in mind. The first was to define regions of the steroid molecule that are important for activity at this nicotinic receptor and to examine the actions of some endogenous neurosteroids. The second was to compare structural requirements for action at the rat neuronal nicotinic  $\alpha 4\beta 2$  receptor with requirements for action at rat hippocampal GABA<sub>A</sub> receptors. This might provide some insight into similarities and differences between the sites on these two related proteins. The final goal was to compare the ability to inhibit nicotinic  $\alpha 4\beta 2$  receptors with the ability of a compound to produce an LRR in *X. laevis*

tadpoles. This comparison would indicate the likelihood that inhibition of this nicotinic receptor is critically involved in producing anesthesia.

The standard assay protocol was to pre-expose a cell to a steroid at a concentration of  $3 \mu\text{M}$  for 30 s. The duration of pre-exposure was chosen based on the onset time course for ACN, and the concentration was chosen because it should reveal compounds that are significantly more or less potent than ACN. Results for the 15 steroids tested are shown in Table 1, structures are presented in Fig. 6, and full chemical names are given in the abbreviations footnote. Results comparing steroid actions on nicotinic receptors, GABA<sub>A</sub> receptors, and tadpole LRR are presented in Table 2.

**Role of 3, 5, and 17 Positions.** Changing the orientation of the 3-OH group (see Fig. 6 for position; compare ACN with B372 in Table 1) or the stereochemistry at carbon 5 ring (part of the A, B-ring fusion; compare ACN with B164 in Fig. 6) had no effect on ability to inhibit acetylcholine elicited responses (compare ACN with B164 in Table 1). This differs from the requirements for potentiation or gating of the GABA<sub>A</sub> receptor. For the GABA<sub>A</sub> receptor, changing the 3-OH group from  $\alpha$ - to  $\beta$ -orientation eliminates potentiation, whereas changing the A, B-ring fusion reduces potentiation. Change at both the 3 and 5 positions slightly but significantly

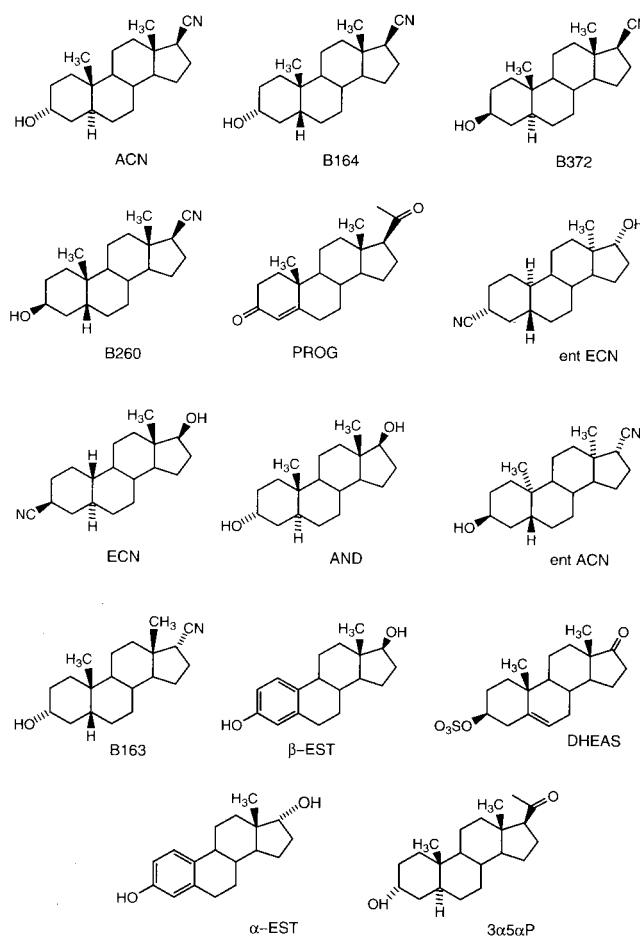


**Fig. 6.** Structures of the steroids tested. The structures of the various steroids tested are shown. The structures are arranged in increasing order of effectiveness at reducing acetylcholine responses (see Table 1), from ACN (top left) to  $3\alpha 5\alpha\text{P}$  (bottom right). Full chemical names are given in the abbreviations footnote.

al., 1998), which also was a weak inhibitor of acetylcholine-elicited responses (Table 1).

Not all steroids were tested for actions on the GABA<sub>A</sub> receptor. However, previous studies have found that progesterone has weak ability to potentiate responses to GABA (Harrison et al., 1987; Wu et al., 1990). Furthermore, although AND can inhibit *t*-butylbicyclophosphorothionate binding to rat cortical sites, it has an IC<sub>50</sub> value of 1 μM compared with 17 nM for 3α5αP (Gee et al., 1988), whereas progesterone is inactive at 10 μM (Hawkinson et al., 1994). Finally, βEST is inactive in inhibiting *t*-butylbicyclophosphorothionate binding at 100 μM (Gee et al., 1987) and actually inhibits GABA-elicited responses from nerve terminals of the posterior pituitary (Zhang and Jackson, 1994). It appears, therefore, that these steroids would have shown minimal potentiating activity for GABA<sub>A</sub> receptors.

We obtained data on the concentration of steroid producing an LRR in half of the *X. laevis* tadpoles exposed to steroid. Because we did not have full nicotinic receptor blocking curves for all compounds, we initially converted the data into ranks for examining correlations. The rank 1 was assigned to the compound producing the most block when used at a steroid concentration of 3  $\mu$ M and correspondingly to the compound that caused LRR at the lowest concentration. The ranks were correlated significantly, with a correlation coefficient of 0.71 and the probability that the coefficient differs from zero of  $P = .007$  (Fig. 8A).

The rank order potency for block of acetylcholine responses and LRR is significant, but the relevance to anesthesia is not clear. This uncertainty arises because the quantitative relationship between potencies for the two actions is not linear. We measured the  $IC_{50}$  value for block of nicotinic responses for five compounds and estimated the  $IC_{50}$  value for an additional nine (Table 1). Figure 8B shows the  $IC_{50}$  values in a logarithmic scatterplot. It is obvious that the concentration needed to produce half-block of the nicotinic response is larger than that necessary to cause LRR. Furthermore, the linear regression coefficient for the logarithmically transformed data is only 0.2, although it differs from a coefficient

### Comparison of steroid actions on nicotinic receptors, GABA<sub>A</sub> receptors, and tadpole LRR

The table is organized with the compound producing the greatest block of nicotinic receptors at the top and that producing the least at the bottom. The first column gives the name of the compound, and the next three columns give the substituent and orientation at the 3, 5, and 17 positions. The column headed "ACh Response" shows the mean residual response to 100  $\mu$ M acetylcholine after preexposure to 3  $\mu$ M steroid (from Table 1). The column headed "GABA Potentiation" gives the relative response of hippocampal neurons to 2  $\mu$ M GABA plus 10  $\mu$ M of the steroid, compared with the response to 2  $\mu$ M GABA alone. A value of 1 indicates no potentiation. The final column gives the IC<sub>50</sub> value for the ability of the compound to produce loss of righting reflex in tadpoles. The data for potentiation shown as (1) are expected results for compounds that have not been tested in this assay but probably would show no potentiation, and B indicates compounds expected to block responses to GABA (see *Results*).

Compound	3	5	17	ACh Response	GABA Potentiation	LRR
ACN	$\alpha$ OH	$\alpha$	$\beta$ CN	0.27	18	0.07
B164	$\alpha$ OH	$\beta$	$\beta$ CN	0.28	13	0.08
B372	$\beta$ OH	$\alpha$	$\beta$ CN	0.33	(1)	0.26
B260	$\beta$ OH	$\beta$	$\beta$ CN	0.46	1.0	0.23
PROG	O	x	$\beta$ CH <sub>3</sub> CO	0.50	(1)	0.22
<i>ent</i> -ECN	$\alpha$ CN	$\beta$	$\alpha$ OH	0.54	1.0	0.84
ECN	$\beta$ CN	$\alpha$	$\beta$ OH	0.56	1.1	0.10
AND	$\alpha$ OH	$\alpha$	$\beta$ OH	0.57	(1)	1.70
<i>ent</i> -ACN	$\beta$ OH	$\beta$	$\alpha$ CN	0.61	2.1	0.59
B163	$\alpha$ OH	$\beta$	$\alpha$ CN	0.66	1.0	9.7
$\beta$ EST	OH	x	$\beta$ OH	0.69	B	17
DHEAS	$\beta$ SO <sub>4</sub>	x	O	0.76	B	N.D.
$\alpha$ EST	OH	x	$\alpha$ OH	0.79	(1)	3.2
3 $\alpha$ 5 $\alpha$ P	$\alpha$ OH	$\alpha$	$\beta$ CH <sub>3</sub> CO	0.84	11	0.42

N.D., not determined.



of zero ( $P = .035$ ). This low value indicates that there is no linear relationship between the potency of steroids at blocking the nicotinic receptor and producing LRR and suggests that LRR is not a simple consequence of block of nicotinic receptors.

## Discussion

**Mechanism of Action of ACN.** These data indicate that the actions of ACN are not mediated by a second messenger pathway, at least one requiring high-energy phosphate compounds or the involvement of GTP-binding proteins. The observed enantioselectivity between ACN and *ent*-ACN indicates that the steroid interacts with a chiral site, rather than intercalating into a bulk hydrophobic milieu to produce the block. Furthermore, the structure-activity data indicate some specificity in interactions between steroid and site. These data suggest that steroids interact with specific sites on the  $\alpha 4\beta 2$  neuronal nicotinic receptor. Previous work has found that ACN does not affect the binding of radiolabeled cytosine to homogenates prepared from these cells (Sabey et al., 1999), which indicates that is not a competitive inhibitor of agonist binding.

Steroids can bind to more than one site on an individual nicotinic receptor, as the Hill coefficient for block is greater than 1 for all the steroids examined. Both the onset and offset of block are slow. The data were analyzed in terms of some simple models, and two were eliminated whereas two were found to provide adequate descriptions of the data. In each case, the better fit was produced when it was assumed that there are relatively few sites on each receptor, in the range of two to five. We were not able to determine whether the slow kinetics of block result primarily from slow association and dissociation or from a slow conformational change after binding.

The present observations support the idea that steroids do

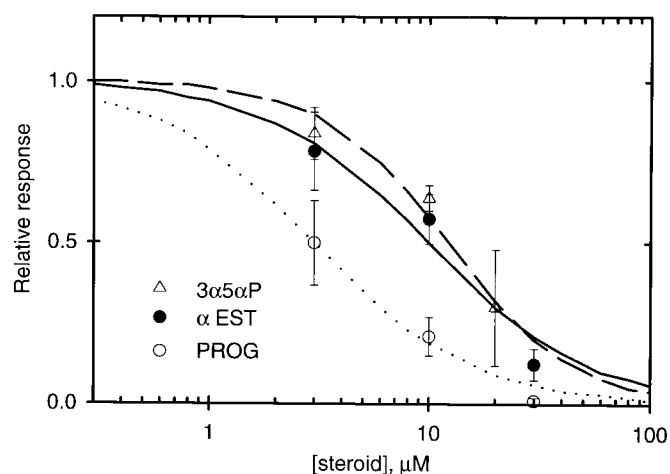


**Fig. 7.** Inhibition by  $\alpha$ EST, PROG, and  $3\alpha 5\alpha$ P. The fraction of control current after a 10- or 30-s application of the various steroids is shown, assayed using 100  $\mu$ M acetylcholine. Data are shown for  $\alpha$ EST (●, solid line), PROG (○, dotted line), and  $3\alpha 5\alpha$ P (△, dashed line). The lines show the fits of eq. 1 to the data with parameters  $IC_{50} = 3.0 \mu$ M,  $n = 1.2$  (PROG),  $IC_{50} = 10 \mu$ M,  $n = 1.2$  ( $\alpha$ EST), and  $IC_{50} = 12.3 \mu$ M and  $n = 1.55$  ( $3\alpha 5\alpha$ P). The fits were made assuming that complete block occurred at high steroid concentrations. Each point shows the arithmetic mean  $\pm$  1 S.D. for data from the following numbers of cells: PROG, 3  $\mu$ M 6, 10  $\mu$ M 4, 30  $\mu$ M 3;  $\alpha$ EST, 3  $\mu$ M 15, 10  $\mu$ M 6, 30  $\mu$ M 4; and  $3\alpha 5\alpha$ P, 3  $\mu$ M 4, 10  $\mu$ M 4, 20  $\mu$ M 8.

not act by altering desensitization of the receptor. Block also develops at a similar rate when ACN is applied alone or in the presence of 1  $\mu$ M acetylcholine, suggesting that block is not strongly selective between resting and active receptors. Overall, the data suggest that steroid interactions with this receptor do not depend strongly on agonist-elicited conformational states of the nicotinic receptor. Steroid binding results in a state that has much reduced activation by acetylcholine. However, the inactivated receptors are not desensitized and can undergo some allosteric transitions (i.e., they can desensitize), so they are not locked in a resting state.

**Comparison of Steroid Structure Important for Actions at Neuronal Nicotinic and GABA<sub>A</sub> Receptors.** There is a clear effect of the stereochemical orientation of the substituent attached at the 17 position, with a  $\beta$ -orientation of either a hydroxyl or carbonitrile group producing more potent nicotinic block than an  $\alpha$ -orientation. This stereoselectivity is qualitatively similar to that for potentiation of responses from GABA<sub>A</sub> receptors. In contrast, the stereochemistry of the A, B-ring fusion or the orientation of the hydroxy group at position 3 has much less of an effect on inhibition of the rat  $\alpha 4\beta 2$  nicotinic receptor than on potentiation of GABA<sub>A</sub> receptors. These comparisons demonstrate

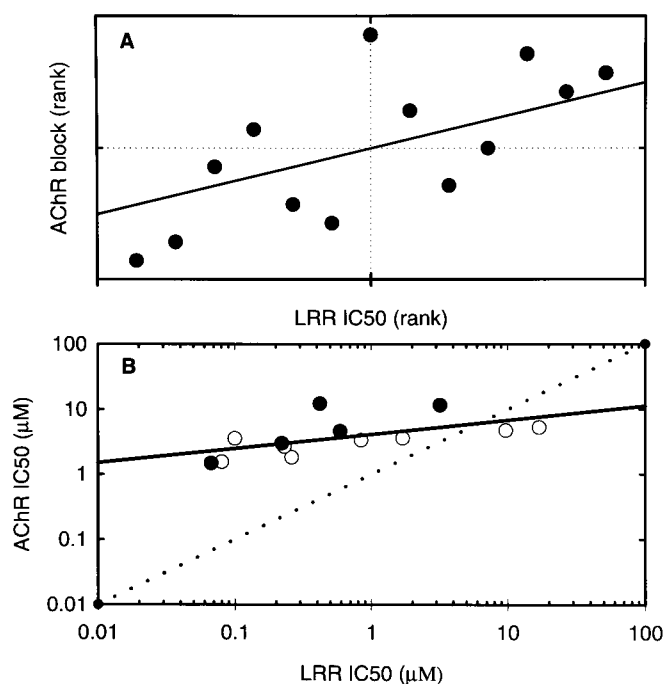


**Fig. 8.** Correlations between inhibition of nicotinic receptors and LRR in tadpoles. A, scatterplot of the rank value for the ability of a compound to block acetylcholine elicited currents (smallest residual current in the presence of 3  $\mu$ M compound is given rank 1) and the rank for ability to cause LRR in tadpoles (smallest  $IC_{50}$  is given rank 1). The linear regression coefficient is 0.71 ( $P = .007$ ), indicating that compounds that produce a greater amount of block are likely to have a greater potency at producing LRR. The line shows the predicted regression relationship (for data values, see Table 1). B, scatterplot of  $IC_{50}$  values (filled symbols measured, open symbols calculated) for the ability of a compound to block acetylcholine-elicited currents and measured  $IC_{50}$  values for ability to cause LRR. Note that both ordinates are logarithmically scaled. The solid line shows the regression relationship for logarithmically transformed data, and the dotted line shows a slope of 1. The linear regression coefficient for logarithmically transformed data is 0.2 ( $P = .035$ ). When only the experimentally determined  $IC_{50}$  values for block of acetylcholine elicited currents are used (filled symbols), the linear regression coefficient for logarithmically transformed data is 0.5 ( $P = .08$ ).

that the interactions between the steroids and the binding site have different structural requirements for neuronal nicotinic receptors and GABA<sub>A</sub> receptors. There are undoubtedly additional features of steroid structure that play a role in the inhibition of rat  $\alpha 4\beta 2$  nicotinic receptors, which may involve both the A and D rings. These are suggested by comparisons between the structure and activity for drugs such as ACN, 3 $\alpha$ 5 $\alpha$ P, and progesterone (see Fig. 6 and Table 1).

**Correlation with Production of LRR in Tadpoles.** There is a strong correlation in the rank orders of the abilities of these compounds to produce anesthesia in *X. laevis* tadpoles (as assayed by the LRR) and the amount of block produced. The correlation suggests that the neuronal nicotinic receptor is involved in production of anesthesia. This simple interpretation is likely inappropriate, because the required concentrations are not linearly related. Three alternative explanations seem more likely. The first is that the rank correlation is simply fortuitous. This seems unlikely, given the statistical significance of the difference of the correlation coefficient from zero. The second is that a single alternative target with similar structural requirements is critical for anesthetic actions. The third possibility is that there are several targets that can result in anesthesia. For example, potentiation of GABA<sub>A</sub> receptor activation might be a primary mechanism. However, for some agents that act weakly at GABA<sub>A</sub> receptors, alternative targets might serve as the molecular substrate for effects leading to LRR (e.g., neuronal nicotinic receptors or voltage-gated calcium channels; Todorovic et al., 1998). Some of the compounds tested in the present study were chosen because they produced LRR with minimal apparent actions on GABA<sub>A</sub> responses (see Table 2), and so the choice of drugs might have emphasized the role of targets other than GABA<sub>A</sub> receptors. In sum, the data indicate that the neuronal nicotinic receptor is not likely to be a primary target by which steroid anesthetic agents produce their behavioral effects. However, block of nicotinic receptors may play a role in the actions of some anesthetic steroids.

**Responses to Neuroactive Steroids Produced In Vivo.** We tested several neuroactive steroids that are present in the rat brain. The compound with the strongest blocking activity is progesterone, with an apparent IC<sub>50</sub> value of about 3  $\mu$ M. The concentration in human cerebrospinal fluid has been estimated to be much lower, about 0.1 nM (Backstrom et al., 1976; Uzunova et al., 1998). There are no comparable data for rat cerebrospinal fluid, but the amount of progesterone in rat brain tissue is about 20 nmol/kg wet wt. (Purdy et al., 1991; Corpechot et al., 1993), whereas the value for human brain is about 100 nmol/kg (Bixo et al., 1997). The concentration of  $\beta$ -estradiol may be even lower: human cerebrospinal fluid concentration is about 0.01 nM (Backstrom et al., 1976), whereas the total brain amount is about 0.2 nmol/kg (female human brain, Bixo et al., 1995; female rat brain, Bixo et al., 1986). It is not certain what the relevant concentration of steroid would be. For example, the free concentration in the cleft might be critical or the concentration in the membrane, and there may be locally increased concentrations of some steroids. However, the bulk concentration in the brain is low compared with the IC<sub>50</sub> values we have measured, which suggests that the rat neuronal nicotinic  $\alpha 4\beta 2$  receptor is unlikely to be significantly modulated by

endogenously produced steroids. It is possible that local high concentrations of steroids may appear in specific brain regions or that longer exposures to steroid might reveal an action on these receptors.

**Other Studies of Steroid Action on Nicotinic Receptors.** Previous studies of neuronal nicotinic receptors have found that chicken  $\alpha 4\beta 2$  receptors, expressed in *X. laevis* oocytes, are inhibited by progesterone with a similar potency as that seen in our studies (Bertrand et al., 1991; Valera et al., 1992), although the Hill coefficient is less than 1. They found that progesterone does not alter desensitization or compete for the agonist binding site, as our results indicate. 3 $\alpha$ 5 $\alpha$ P could produce only a partial block of responses from these chicken receptors even at maximally effective doses (Bertrand et al., 1991). In our hands, 3 $\alpha$ 5 $\alpha$ P could produce full block of rat  $\alpha 4\beta 2$  receptors, although with lower potency than progesterone. Ion fluxes in SH-SY5Y cells (likely expressing neuronal nicotinic receptors containing  $\alpha 3$  and  $\beta 4$  subunits) also are inhibited by progesterone with an IC<sub>50</sub> value of 11  $\mu$ M (Ke and Lukas, 1996). In both of these studies, progesterone covalently coupled to bovine serum albumin was effective at inhibition, indicating that the steroid can reach its site directly from the bathing solution.

Muscle nicotinic receptors also are blocked by a number of steroids. The anesthetic steroid alfaxalone was proposed to block responses by a selective block of active receptors (Gillo and Lass, 1984). Corticosteroids have been shown to reduce the mean open time for muscle nicotinic receptors (Bouzat and Barrantes, 1996; Nurowska and Ruzzier, 1996), although apparently not via an open channel blocking mechanism (Bouzat and Barrantes, 1996). A recent study examined promegestone inhibition of nicotinic receptor of *Torpedo* electroplex (Blanton et al., 1999). Promegestone appeared to enhance desensitization. One region for interaction between promegestone and the *Torpedo* receptor was the membrane spanning helix M4 of all four subunits, as determined by photolabeling of the proteins (Blanton et al., 1999). In contrast, a study of the interaction of spin-labeled lipids with *Torpedo* receptors found that the immobilization of an analog of AND was removed when the extramembranous portions of the protein were digested with proteases, whereas the immobilization of a phospholipid analog was unaffected (Dreger et al., 1997). The results were interpreted to indicate that the interactions between this steroid and receptor occurred, at least in part, outside the lipid bilayer. Overall, the data suggest that there are some differences in the action of steroids on neuronal and muscle-type nicotinic receptors.

Glycine receptors in cultured chick spinal cord neurons are also inhibited by progesterone and DHEAS (Wu et al., 1990), whereas 3 $\alpha$ 5 $\alpha$ P has minimal effects on glycine receptors in chick spinal cord cells (Wu et al., 1990) or expressed in *Xenopus* oocytes (Pistis et al., 1997). In a qualitative sense, therefore, the structural requirements for inhibition of neuronal nicotinic receptors and glycine receptors may be more similar to each other than to those for GABA<sub>A</sub> receptor potentiation.

#### Acknowledgments

We thank Jessie Zhang for culturing cells, Dr. Mingcheng Han for synthesizing some steroids used in these studies, and Devi Nathan and Melissa Kalkbrenner for performing the tadpole LRR studies.

## References

- Backstrom T, Carstensen H and Sodergard R (1976) Progesterone in cerebrospinal fluid compared to plasma unbound and total concentrations. *J Steroid Biochem* **7**:469–472.
- Bertrand D, Valera S, Bertrand S, Ballivet M and Rungger D (1991) Steroids inhibit nicotinic acetylcholine receptors. *Neuroreport* **2**:277–280.
- Bixo M, Andersson A, Winblad B, Purdy RH and Backstrom T (1997) Progesterone, 5 $\alpha$ -pregnane-3,20-dione and 3 $\alpha$ -hydroxy-5 $\alpha$ -pregnane-20-one in specific regions of the human female brain in different endocrine states. *Brain Res* **764**:173–178.
- Bixo M, Backstrom T, Winblad B and Andersson A (1995) Estradiol and testosterone in specific regions of the human female brain in different endocrine states. *J Steroid Biochem Mol Biol* **55**:297–303.
- Bixo M, Backstrom T, Winblad B, Selstam G and Andersson A (1986) Comparison of pre- and postovulatory distributions of oestradiol and progesterone in the brain of PMSG-treated rats. *Acta Physiol Scand* **128**:241–246.
- Blanton MP, Xie Y, Dangott LJ and Cohen JB (1999) The steroid progesterone is a noncompetitive antagonist of the *Torpedo* nicotinic acetylcholine receptor that interacts with the lipid-protein interface. *Mol Pharmacol* **55**:269–278.
- Bouzat C and Barrantes FJ (1996) Modulation of muscle nicotinic acetylcholine receptors by the glucocorticoid hydrocortisone: Possible allosteric mechanism of channel blockade. *J Biol Chem* **271**:25835–25841.
- Corpechot C, Young J, Calvel M, Wehrey C, Veltz JN, Touyer G, Mouren M, Prasad VV, Banner C, Sjoval J, Baulieu EE and Robel P (1993) Neurosteroids: 3 $\alpha$ -Hydroxy-5 $\alpha$ -pregnan-20-one and its precursors in the brain plasma and steroidogenic glands of male and female rats. *Endocrinology* **133**:1003–1009.
- Dreger M, Krauss M, Herrmann A and Hucho F (1997) Interactions of the nicotinic acetylcholine receptor transmembrane segments with the lipid bilayer in native receptor-rich membranes. *Biochemistry* **36**:839–847.
- Flood P, Ramirez-Latorre J and Role L (1997)  $\alpha 4\beta 2$  Neuronal nicotinic acetylcholine receptors in the central nervous system are inhibited by isoflurane and propofol but  $\alpha 7$ -type nicotinic acetylcholine receptors are unaffected. *Anesthesiology* **86**:859–865.
- Franks NP and Lieb WR (1993) Selective actions of volatile general anaesthetics at molecular and cellular levels. *Br J Anaesth* **71**:65–76.
- Gee KW, Bolger MB, Brinton RE, Coirini H and McEwen BS (1988) Steroid modulation of the chloride ionophore in rat brain: Structure-activity requirements regional dependence and mechanism of action. *J Pharmacol Exp Ther* **246**:803–812.
- Gee KW, Chang WC, Brinton RE and McEwen BS (1987) GABA-dependent modulation of the Cl<sup>−</sup> ionophore by steroids in rat brain. *Eur J Pharmacol* **136**:419–423.
- Gillo B and Lass Y (1984) The mechanism of steroid anaesthetic (alphaxalone) block of acetylcholine-induced ionic currents. *Br J Pharmacol* **82**:783–789.
- Harrison NL, Majewska MD, Harrington JW and Barker JL (1987) Structure-activity relationships for steroid interaction with the  $\beta$ -aminobutyric acid A receptor complex. *J Pharmacol Exp Ther* **241**:346–353.
- Hawkinson JE, Kimbrough CL, Belelli D, Lambert JJ, Purdy RH and Lan NC (1994) Correlation of neuroactive steroid modulation of [<sup>35</sup>S]*t*-butylbicyclophosphorothionate and [<sup>3</sup>H]flunitrazepam binding and  $\gamma$ -aminobutyric acid A receptor function. *Mol Pharmacol* **46**:977–985.
- Ke L and Lukas RJ (1996) Effects of steroid exposure on ligand binding and functional activities of diverse nicotinic acetylcholine receptor subtypes. *J Neurochem* **67**:1100–1112.
- Lambert JJ, Belelli D, Hill-Venning C and Peters JA (1995) Neurosteroids and GABA<sub>A</sub> receptor function. *Trends Pharmacol Sci* **16**:295–303.
- Majewska MD and Schwartz RD (1987) Pregnenolone-sulfate: An endogenous antagonist of the  $\gamma$ -aminobutyric acid receptor complex in brain? *Brain Res* **404**:355–360.
- McGehee DS and Role LW (1996) Presynaptic ionotropic receptors. *Curr Opin Neurobiol* **6**:342–349.
- Nilsson KR, Zorumski CF and Covey DF (1998) Neurosteroid analogues. 6. The synthesis and GABA<sub>A</sub> receptor pharmacology of enantiomers of dehydroepiandrosterone sulfate pregnenolone sulfate and (3 $\alpha$ 5 $\beta$ )-3-hydroxypregnan-20-one sulfate. *J Med Chem* **41**:2604–2613.
- Nurowska E and Ruzzier F (1996) Corticosterone modifies the murine muscle acetylcholine receptor channel kinetics. *Neuroreport* **8**:77–80.
- Park-Chung M, Wu FS, Purdy RH, Malayev AA, Gibbs TT and Farb DH (1997) Distinct sites for inverse modulation of *N*-methyl-D-aspartate receptors by sulfated steroids. *Mol Pharmacol* **52**:1113–1123.
- Pistis M, Belelli D, Peters JA and Lambert JJ (1997) The interaction of general anaesthetics with recombinant GABA<sub>A</sub> and glycine receptors expressed in *Xenopus laevis* oocytes: A comparative study. *Br J Pharmacol* **122**:1707–1719.
- Purdy RH, Morrow AL, Moore PH Jr and Paul SM (1991) Stress-induced elevations of  $\gamma$ -aminobutyric acid type A receptor-active steroids in the rat brain. *Proc Natl Acad Sci USA* **88**:4553–4557.
- Role LW and Berg DK (1996) Nicotinic receptors in the development and modulation of CNS synapses. *Neuron* **16**:1077–1085.
- Sabey K, Paradiso K, Zhang J and Steinbach JH (1999) Ligand binding and activation of rat nicotinic  $\alpha 4\beta 2$  receptors stably expressed in HEK 293 cells. *Mol Pharmacol* **55**:58–66.
- Todorovic SM, Prakriya M, Nakashima YM, Nilsson KR, Han M, Zorumski CF, Covey DF and Lingle CJ (1998) Enantioselective blockade of T-type Ca<sup>2+</sup> current in adult rat sensory neurons by a steroid that lacks  $\beta$ -aminobutyric acid-modulatory activity. *Mol Pharmacol* **54**:918–927.
- Tonner PH, Poppers DM and Miller KW (1992) The general anesthetic potency of propofol and its dependence on hydrostatic pressure. *Anesthesiology* **77**:926–931.
- Uzunova V, Sheline Y, Davis JM, Rasmusson A, Uzunov DP, Costa E and Guidotti A (1998) Increase in the cerebrospinal fluid content of neurosteroids in patients with unipolar major depression who are receiving fluoxetine or fluvoxamine. *Proc Natl Acad Sci USA* **95**:3239–3244.
- Valera S, Ballivet M and Bertrand D (1992) Progesterone modulates a neuronal nicotinic acetylcholine receptor. *Proc Natl Acad Sci USA* **89**:9949–9953.
- Violet JM, Downie DL, Nakisa RC, Lieb WR and Franks NP (1997) Differential sensitivities of mammalian neuronal and muscle nicotinic acetylcholine receptors to general anaesthetics. *Anesthesiology* **86**:866–874.
- Wittmer LL, Hu YF, Kalkbrenner M, Evers AS, Zorumski CF and Covey DF (1996) Enantioselectivity of steroid-induced  $\gamma$ -aminobutyric acid A receptor modulation and anesthesia. *Mol Pharmacol* **50**:1581–1586.
- Wu FS, Gibbs TT and Farb DH (1990) Inverse modulation of  $\gamma$ -aminobutyric acid- and glycine-induced currents by progesterone. *Mol Pharmacol* **37**:597–602.
- Zhang SJ and Jackson MB (1994) Neuroactive steroids modulate GABA<sub>A</sub> receptors in peptidergic nerve terminals. *J Neuroendocrinol* **6**:533–538.

**Send reprint requests to:** Dr. Joe Henry Steinbach, Department of Anesthesiology, Washington University School of Medicine, 660 South Euclid Avenue, St. Louis, MO 63110. E-mail: jhs@morpheus.wustl.edu